International Gas Turbine Conference 2015 Tokyo
November 15(Sun.)-20(Fri.), 2015

IGTC-2015-20

Investigation of Unsteady Flow Interaction between an Ultra-Compact Inlet and a Transonic Fan

Chunill Hah[1], Douglas Rabe[2] and Angie Scribben[2]

[1] NASA Glenn Research Center
MS 5-11, Cleveland, Ohio 44135
[2] AFRL, WPAFB, Ohio 45433

ABSTRACT

In the study presented, unsteady flow interaction between an ultra-compact inlet and a transonic fan stage is investigated. Future combat aircraft engines require ultra-compact inlet ducts as part of an integrated, advanced propulsion system to improve air vehicle capability and effectiveness to meet future mission needs. The main purpose of the current study is to advance the understanding of the flow interaction between a modern ultra-compact inlet and a transonic fan for future design applications. Many experimental/analytical studies have been reported on the aerodynamics of compact inlets in aircraft engines. On the other hand, very few studies have been reported on the effects of flow distortion from these inlets on the performance of the following fan/compressor stages. The primary goal of the study presented is to investigate how flow interaction between an ultra-compact inlet and a transonic compressor influence the operating margin of the compressor. Both Unsteady Reynolds-averaged Navier-Stokes (URANS) and Large Eddy Simulation (LES) approaches are used to calculate the unsteady flow field, and the numerical results are used to study the flow interaction. The present study indicates that stall inception of the following compressor stage is affected directly based on how the distortion pattern evolves before it interacts with the fan/compressor face. For the present compressor, the stall initiates at the tip section with clean inlet flow and distortion pattern away from the casing itself seems to have limited impacts on the stall inception of the compressor. A counter-rotating swirl, which is generated due to flow separation inside the s-shaped compact duct, generates an increased flow angle near the blade tip. This increased flow angle near the rotor tip due to the secondary flow from the counter-rotating vortices is the primary reason for the reduced compressor stall margin.

INTRODUCTION

Ultra-compact inlets are being increasingly used for certain types of aircraft. As the total pressure distortion from such an inlet affects the total performance of the propulsion system, various studies have been conducted to control/minimize the total pressure distortion from compact inlets. However, very few studies have been reported on the interaction of compact inlets with the following fan/compressor stages.

Many experimental/analytical studies have been reported on the effects of various inlet flow distortions on transonic compressor flow fields. Horlock (1968) presented some fundamental methods to estimate changes in blade loading due to the total pressure distortion. Monsarat (1968) reported an experimental investigation on the effects of inlet total pressure distortion on a hig hly loaded transonic compressor. Bowditch et al. (1988) reported an experimental study on the effects of inlet total pressure distortion on the compressor operating margin. Rabe et al. (1995) studied blade response to the inlet total pressure distortion with miniature pressure transducers mounted on the rotor blade in a highly loaded modern transonic compressor stage. Hah et al. (1996) investigated effects of inlet distortion on the flow field in a transonic compressor rotor with both measurement and numerical analysis. The inlet distortion was generated by a distortion screen with various distortion patterns.

Figure 1: Inlet/fan test rig.

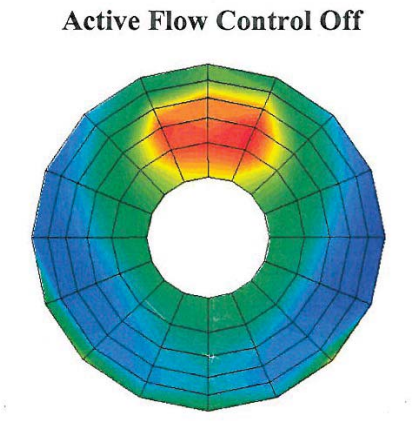

Figure 2: Measured total pressure distribution at AIP

Figure 3: Simplified inlet/fan configuration

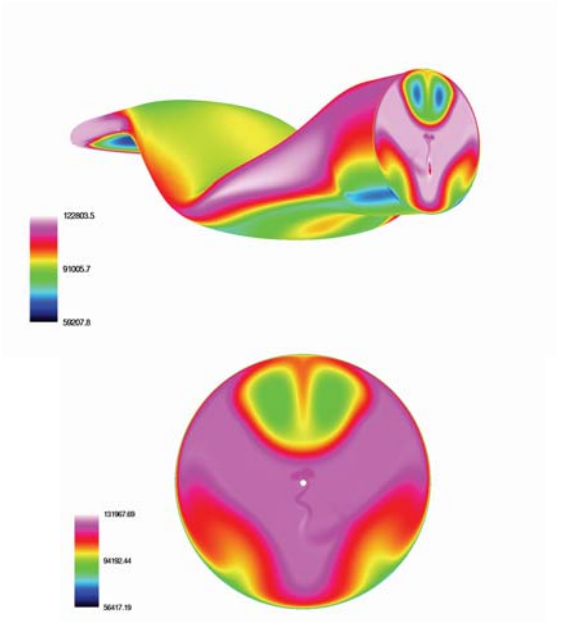

Figure 4: Calculated total pressure distribution

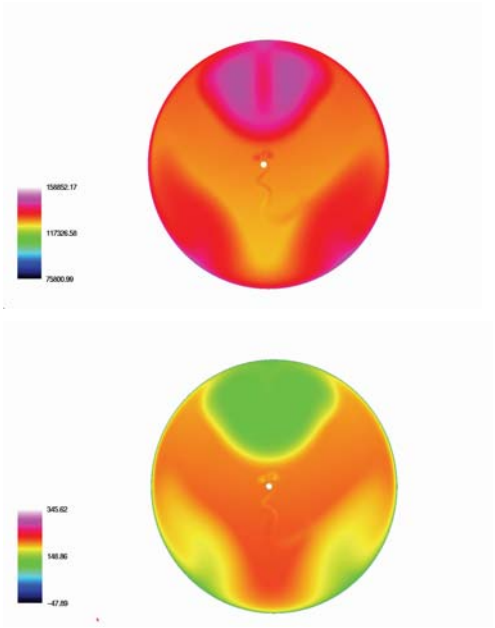

Figure 5: Calculated total temperature and axial velocity distribution at AIP.

With the development of boundary ingesting intakes for the next generation of aircraft design, several studies on flow through serpentine inlets with boundary layer ingestion have been reported. Plas et al. (2007) studied the effects of duct geometry on the distortion pattern at the duct exit. Madani and Hynes (2009) studied duct contours on the exit distortion pattern. Defoe and Spakovszky (2012) investigated the effects of boundary layer ingestion on the aero-acoustics of transonic fan rotors both analytically and numerically.

The primary focus of this study is to investigate how the distortion pattern from the compact inlet affects the stall margin of the following transonic compressor. Unsteady flow fields obtained with URANS and LES are used for the current study.

OVERALL GOAL AND ENGINE TEST PROGRAM

The Versatile Active Integrated Inlet/Fan for Performance and Durability Project (VAIIPR) was conducted at the Air Force Research Lab (AFRL). The program was aimed at maturing active flow control technology for an advanced serpentine inlet system integrated in a typical turbofan engine. The main tasks were reducing total pressure distortion and pressure-based harmonics related to fan blade excitation from the serpentine inlet with the flow control technology. The main tasks were accomplished and demonstrated through the program. Figure 1 shows the inlet/fan test rig installed at the AFRL. Measured distribution of the total pressure at the aerodynamic interaction plane (AIP) is shown in Figure 2. The measurements show a low total pressure region near the top section of the AIP plane. The center of this distortion pattern is located at about 65% of the span. As a part of the technology program, an active flow control (AFC) was applied to reduce flow distortion at the exit of the serpentine inlet. The applied AFC decreases the total pressure distortion by about 70%, which results in a significant increase in pressure recovery and a drastic decrease in fan blade deflection. Various tests were conducted to study the effects of the inlet-generated distortion on the operating range of the following fan. The measurements showed a small change in the fan operating margin due to the inlet flow distortion. One of the possible causes of this observation could be the relatively large spacing between the AIP and the fan face for the test set-up. The present study is motivated to investigate detailed flow interactions between the ultra-compact inlet, the fan, and the impact on the fan stall margin. A relatively simple configuration with the same serpentine inlet and the fan blade from the engine test was selected, and a detailed numerical study was conducted for the inlet/fan interaction study. Figure 3 shows the simplified inlet/fan configuration. The fan has 22 radial blades, and the inlet's relative Mach is about 1.4 at design condition. The distance from the AIP to the fan face is 60% of the fan diameter.

NUMERICAL PROCEDURE

Both URANS and LES methods are applied in the presented study. URANS was first applied to obtain the fan speed line and to compare the overall flow structures at various operating conditions with the measured data. The LES procedure was applied primarily to examine the unsteady interaction of the distorted inlet flow with the fan blade. A standard two-equation turbulence model was used for the URANS. A Smagorinsky-type eddy-viscosity model was used for the subgrid stress tensor, and the standard dynamic model by Germano et al. [1991] was applied for the LES. In the current study, the governing equations are solved with a pressure-based implicit method using a fully conservative control volume approach. A third-order accurate interpolation scheme is used for the discretization of convection terms and central differencing is used for the diffusion terms. The method is of second-order accuracy with smoothly varying grids. For the time-dependent terms, an implicit second-order scheme is used and a number of sub-iterations are performed at each time step. Details of the numerical method and applications to transonic flows are given by Hah and Shin [2012].

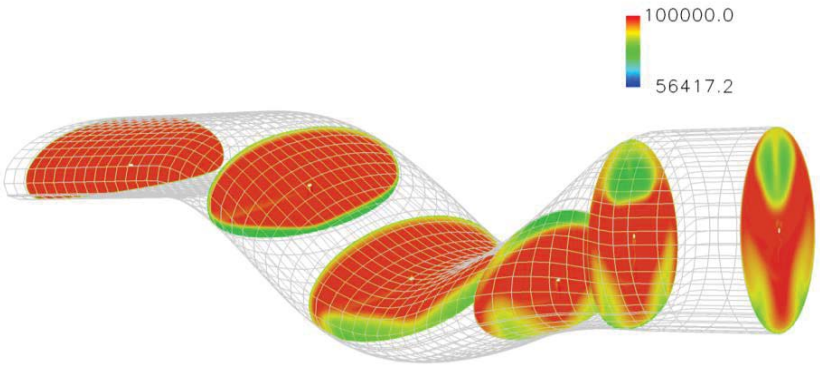

Figure 6: Development of static pressure through the inlet.

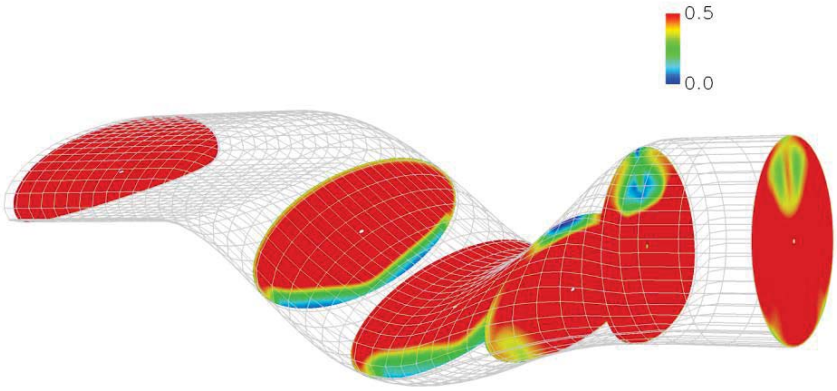

Figure 7: Development of Mach number through the inlet.

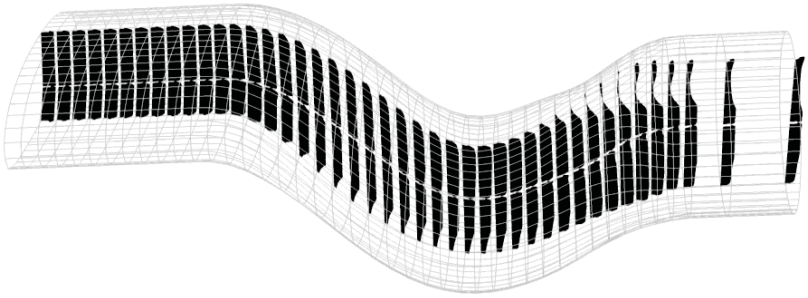

Figure 8: Development of velocity vectors at the symmetry line of the inlet.

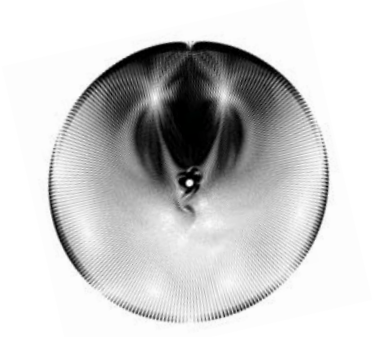

Figure 9: Instantaneous velocity vectors at AIP.

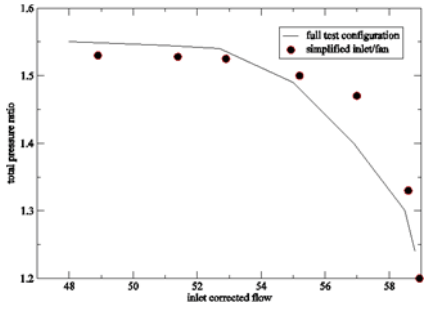

Figure 10: Pressure rise characteristics of fan.

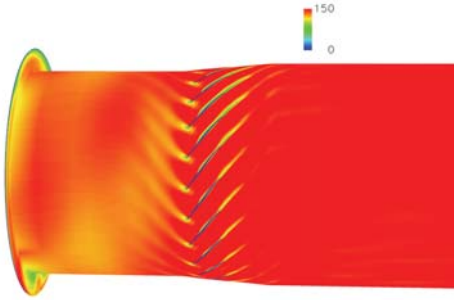

Figure 11: Instantaneous axial velocity contours at 65% span, near stall operation

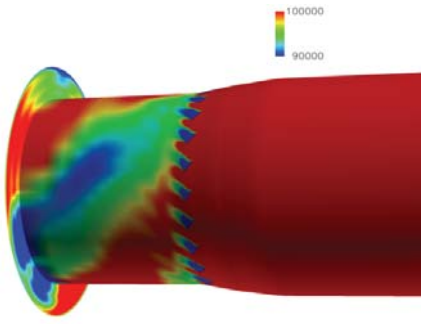

Figure 12: Instantaneous total pressure distribution at 65% span, near stall operation

About 900,000 nodes were applied to the single-passage analysis of the fan with a clean inlet. For the coupled inlet/fan analysis, about 40,000,000 nodes were applied for the inlet and full annulus of the fan. The inflow boundary was located at the entrance of the inlet and the outflow boundary was located three blade heights from the trailing edge of the fan. The rotor tip clearance geometry is accurately represented by 16 nodes in the blade-to-blade direction, 20 nodes in the spanwise direction, and 140 nodes in the streamwise direction. I-grid topology is used to reduce grid skewness and a single-block grid is used. All the computations were performed with NASA's Pleiades supercomputer system, which allows parallel computation with up to 512 processors.

Constant total pressure and total temperature conditions, along with axial flow, were applied at the inlet. Circumferentially averaged static pressure at the casing was specified to control the mass flow rate. Non-reflecting boundary conditions were applied at the inlet and exit boundaries.

FLOW DEVELOPMENT THROUGH INLET

Calculated instantaneous total pressure distribution near the casing of and at the exit of the serpentine inlet is shown in Figure 4. The total pressure distortion pattern at the AIP in Figure 4 matches well with the measurement shown in Figure 2. The total pressure distortion at the AIP originates from the flow separation near the casing of the inlet and instantaneous distribution of the total pressure is not symmetric. Figure 5 shows calculated distributions of total temperature and axial velocity at the AIP. Development of static pressure and the Mach number through the inlet are given in Figures 6 and 7. As shown in Figures 6 and 7, flow distortion originates from the flow separation near the casing where flow decelerates due to the sudden change in curvature. Figure 8 shows the distribution of velocity vectors at the center symmetry plane of the inlet. The flow near the upper casing of the inlet separates after the bend, which creates two counter-rotating vortices at the AIP. The flow near the lower casing decelerates near the bend without flow separation, which results in two weak vortices at the AIP. Instantaneous velocity vectors on the AIP are shown in Figure 9. The center of two counter-rotating vortices is located at about 60% span. The flow incidence angle is expected to be increased or decreased due to tangential components of the vortices as the distortion pattern approaches the fan blade.

INTERACTION BETWEEN INLET AND TRANSONIC FAN

The calculated pressure rise characteristic of the fan is shown in Figure 10. In Figure 10, measured total pressure rise characteristics of the full test rig at 80% are also given. The simplified inlet/fan configuration gives slightly smaller operating margins compared to the full test rig. The numerical results are investigated to determine changes in flow structure by the inlet flow distortion at near stall condition. Instantaneous distribution of axial velocity at 65% span is shown in Figure 11. The calculated instantaneous distribution of total pressure from the AIP to the fan at 65% span is shown in Figure 12. As shown in Figure 12, the total pressure distribution pattern covers about 3 blade passages. The flow incidence angle varies in the circumferential direction due to the two counter-rotating vortices, as shown in Figure 10. Total pressure contours in Figure 12 show that the shocks near the leading edge are stronger where the distortion vortices interact with the blade. The axial velocity contours in Figure 11 indicates that the leading edge shock is moved further ahead of the blade where the low momentum area meets the fan blade. Also, the blade boundary layer on the suction surface and the wake are significantly bigger in this area compared to the area where clean inlet flow meets the fan blade. The difference in the leading edge shock system and the resulting difference in the boundary layer development confirm that blade stall will initiate from the blade passages where the distortion vortices interact with the fan blade.

Figure 13 shows changes in static pressure at three equal-

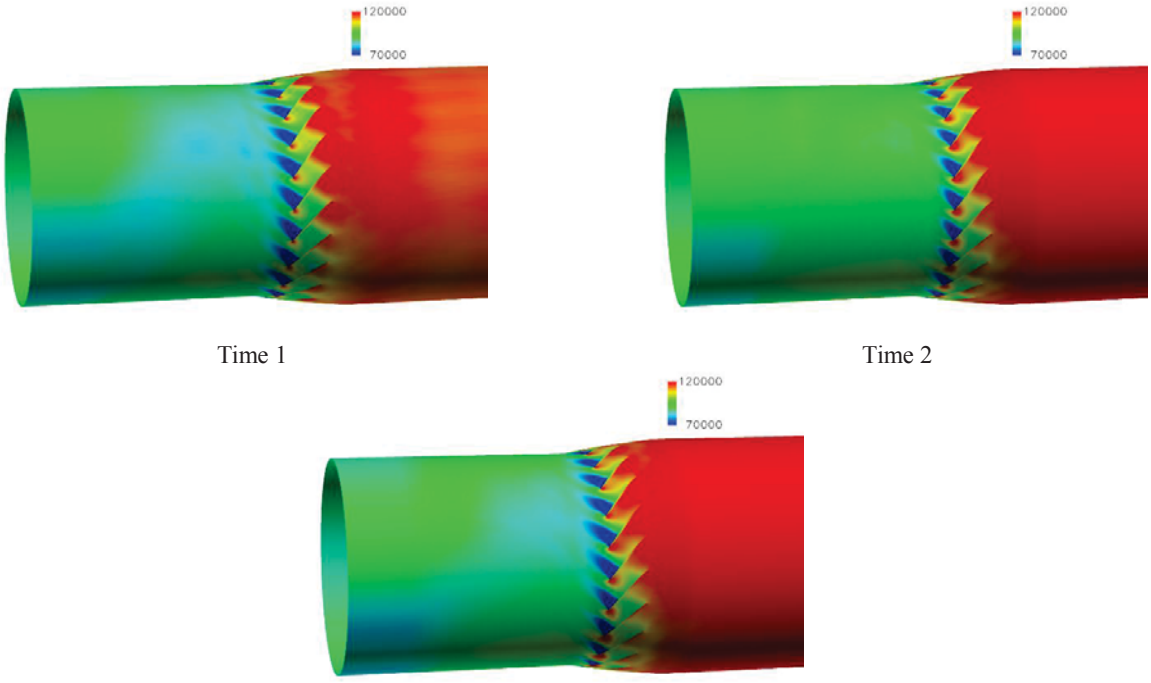

Time 1 Time 2

Time 3

Figure 13: Instantaneous static pressure contours at three times, 65% span, near stall.

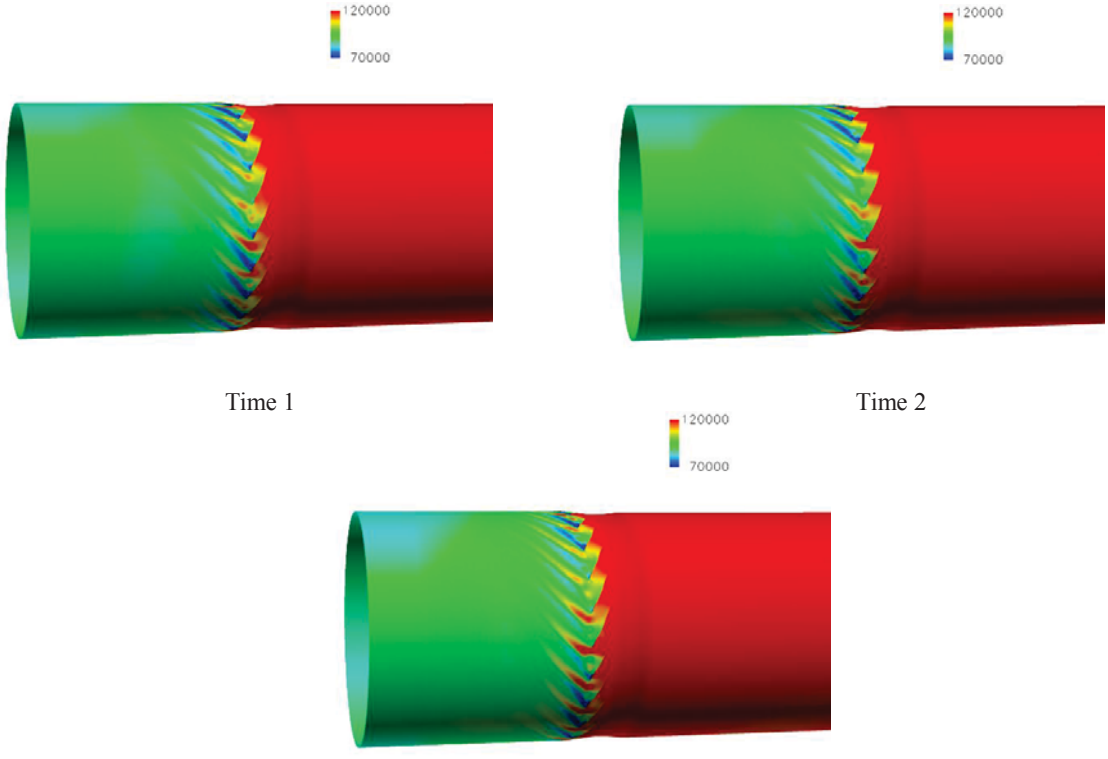

Time 1 Time 2

Time 3

Figure 14: Instantaneous static pressure contours at three times, rotor tip, near stall.

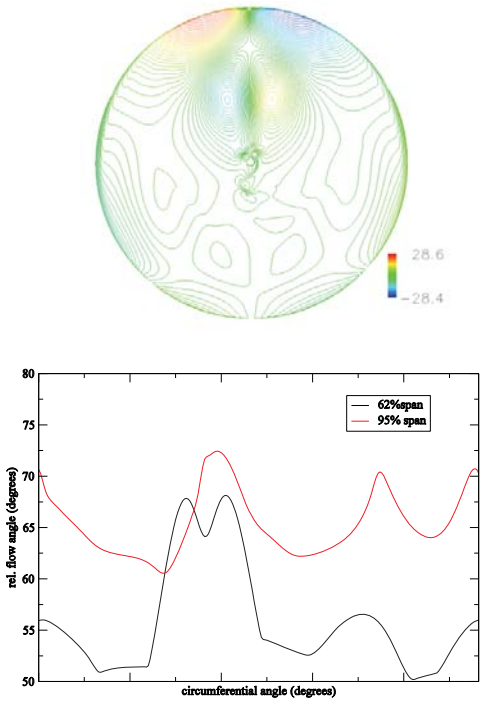

Figure 15: Circumferential distribution of inflow angle at 65% and 95% span.

ly-spaced times at 65% span as the fan enters an unstable operating condition. The shock structures are very similar to what is shown in Figure 12, and the flow structure does not change at this span where the center of counter-rotating vortices interact with the fan blade. Changes in shock structure at the rotor tip at the same times are given in Figure 14. At the rotor tip, flows near the leading edge of several blade passages begin to stall while the flow structures at 65% span are still healthy. Results in Figures 14 and 15 show that the stall inception initiates at the rotor tip, and not at 65% span where the center of distortion vortices hit the fan blade.

The distortion changes the local operating condition as it approaches the fan because the local flow incidence angle varies across the distortion pattern. Changes in the instantaneous local flow angle at 65% span and at the rotor tip are given in Figure 15. The flow angle changes much more at the rotor tip compared to those at 65% span. The large increase/decrease in flow angle at the rotor tip is due to the large tangential velocity components generated by the counter-rotating vortices in the distortion pattern. At the center of the vortices, the total pressure becomes lower. However, the flow incidence does not increase proportionally. At near 65% span, radial velocity is increased or decreased due to the secondary velocity field from the counter-rotating vortices as shown in Figure 9. As the instantaneous flow incidence increases significantly due to the distorted inflow at the rotor tip, stall inception initiates at the rotor tip instead of at 65% span where the center of distortion vortices interact with the blade. The effects of the serpentine-inlet/fan interaction are directly dependent on the fan's design, as well as the radial loading distribution of the fan.

CONCLUDING REMAKRS

Flow interaction between an ultra-compact-serpentine inlet and a transonic fan was studied with both URANS and LES. Calculated flow fields were compared with the available measured data. The primary focus of the present study is to determine how the distorted flow from the serpentine inlet affects the operating range of the fan/compressor stage. A simple configuration of a serpentine inlet and a transonic fan was selected for the detailed numerical investigation. A distortion pattern is developed at the exit of the inlet due to flow separation and deceleration at bends of the inlet. The main feature of the distortion pattern is the counter-rotating vortices whose center is located at about 65% span on the AIP. The tangential velocity component changes the flow incidence angle as the distortion pattern interacts with the fan face. As expected, the blade passage shock at the leading edge becomes stronger and moves further upstream where the low momentum area on the distortion pattern hits the fan blade. Detailed examination of the instantaneous flow structures are at 65% span, where the counter-rotating vortices interact with the blade, and at the rotor tip, where the actual stall initiates at the rotor tip section. Instantaneous distribution of the flow angle indicates that a large increase in the flow incidence angle is observed near the rotor tip due to this counter-rotating vortex system. Further investigations are needed to examine the effects of the distance between the AIP and the fan face, as well as the design of the fan, specifically spanwise distribution of aerodynamic loading.

ACKNOWLEDGEMENTS

The authors gratefully acknowledge the support of this work by the NASA Fundamental Aeronautics program, High Speed project.

REFERENCES

Bowditch, D.N. and Coltrin, R.E., 1983, "A Survey of Engine Inlet Distortion Capability," NASA TM-83421.

Defoe, J.J, and Spakovszky, Z.S., 2012, "Effects of Boundary Layer Ingestion on the Aero-Acoustics of Transonic Fan Rotors," ASME Paper GT2012-68503.

Germano, M., Piomelli, U., Moin, P., and Cabot, W. H., 1991, "A Dynamic Subgrid-Scale Eddy-Viscosity Model," Journal of Fluid Mechanics, Vol. A3, pp. 170-176.

Hah, C., Rabe, D.C., Sullivan, T.J., and Wadia, A.R., 1996, "Effects of Inlet Distortion on the Flow Field in a Transonic Compressor Rotor," ASME Journal of Turbomachinery, Vol.120, No.2, pp.233-246.

Hah, C. and Shin, H., 2012, "Study of Near-Stall Flow Behavior in a Modern Transonic Fan with Compound Sweep," ASME Journal of Fluid Engineering, Vol. 134, pp. 1-7.

Horlock, J.H., 1968, "Fluctuating Lifting Forces on Airfoils moving through Transverse and Chordwise Gusts," ASME Journal of Basic Engineering, 68-FE-28.

Madani, V. and Hynes, T., 2009, "Boundaru Layer Ingesting Intakes: Design and Optimization," ISABE paper ISABE-2009-1346.

Monsarrat, N.T., 1969, "Design Report: Single-Stage Evaluation of Highly-Loaded High-Mach-Number Compressor Stage," NASA CR 72562.

Plas, A., Sargeant, M., Mdani, V., Chrichton, D., Greitzer, E., Hynes T., and Hall, C., 2007, "Performance of a Boundary-Ingesting (BLI) Propulsion Systems," AIAA Paper 2007-450.

Rabe, D., Bolcs, A., and Russler, P., 1995, "Influence of Inlet Distortion on Transonic Compressor Blade Loading," AIAA Paper 95-2461.